Nanoscale

Cite this: *Nanoscale*, 2011, **3**, 1127

www.rsc.org/nanoscale

PAPER

Irreversible changes in protein conformation due to interaction with superparamagnetic iron oxide nanoparticles

Morteza Mahmoudi,*[a] Mohammad A. Shokrgozar,[a] Soroush Sardari,[b] Mojgan K. Moghadam,[a] Hojatollah Vali,[e] Sophie Laurent[c] and Pieter Stroeve[d]

Received 30th September 2010, Accepted 19th November 2010
DOI: 10.1039/c0nr00733a

The understanding of the interactions between nanomaterials and proteins is of extreme importance in medicine. In a biological fluid, proteins can adsorb and associate with nanoparticles, which can have significant impact on the biological behavior of the proteins and the nanoparticles. We report here on the interactions of iron saturated human transferrin protein with both bare and polyvinyl alcohol coated superparamagnetic iron oxide nanoparticles (SPIONs). The exposure of human transferrin to SPIONs results in the release of iron, which changes the main function of the protein, which is the transport of iron among cells. After removal of the magnetic nanoparticles, the original protein conformation is not recovered, indicating irreversible changes in transferrin conformation: from a compact to an open structure.

1 Introduction

Interest in nanoparticles arises from the fact that the mechanical, chemical, electrical, optical, magnetic, electro-optical and magneto-optical properties of these particles are different from their bulk properties and depend on particle size.[1–6] There are numerous areas where nanoparticulate systems are of scientific and technological interest, specifically for biomedicine where the synthesis and biology come together (*i.e.* the nano-biointerface) and lead to an important concern for design of safe nano-biomaterials. A significant challenge for the safety of nanoparticles for biomedical use, such as diagnosis and therapeutics, is that human plasma proteins can be adsorbed on nanoparticles which can cause the transmittance of biological effects due to altered protein conformation.[7–11] More specifically, identification of the adsorbed proteins and evaluation of their lifetime on the surface of nanoparticles are very important and can affect protein–nanoparticle interactions.[12–14] The conformational changes of the proteins can modify their functions, which are recognized as the molecular mechanisms of injury, and could contribute to disease pathogenesis.[13,15–18]

[a]National Cell Bank, Pasteur Institute of Iran, #69 Pasteur Ave., Tehran, 13164, Iran. E-mail: Mahmoudi@biospion.com; Web: www.biospion.com
[b]Department of Medical Biotechnology, Biotechnology Research Center, Pasteur Institute of Iran, #69 Pasteur Ave., Tehran, 13164, Iran
[c]Department of General, Organic, and Biomedical Chemistry, NMR and Molecular Imaging Laboratory, University of Mons, Avenue Maistriau, 19, B-7000 Mons, Belgium
[d]Department of Chemical Engineering and Materials Science, University of California Davis, Davis, USA
[e]Department of Anatomy and Cell Biology and Facility for Electron Microscopy Research, McGill University, Montréal, QC, Canada , H3A 2B2

Lynch *et al.*[19] hypothesized that the function and fate of nanoparticles in biological environments are not only related to the nanoparticle in itself, but also related to its surface protein corona, with various binding affinities. It has been well-recognized that the protein corona covers the surface of nanoparticles upon their entrance into the bloodstream.[7,11] The protein modified surface of the nanoparticles is recognised by living cells, and is a key phenomenon that scientists need to understand.[15,19]

The biological responses to nanoparticles are highly affected by the resultant of main forces at the nano-biointerface (*e.g.*, hydrodynamic, electrodynamic, electrostatic, solvent, steric, and polymer bridging) but also by the characteristics of the nanoparticles (size, shape, charge, crystallinity, electronic states, surface wrapping in the biological medium, hydrophobicity and wettability).[15,20–22] Therefore, a better understanding of the nanoparticle–protein complex is essential in order to develop functional as well as safe nanoparticles.

Among various types of nanoparticles which are used for biomedical applications, superparamagnetic iron oxide nanoparticles (SPIONs) have received increased attention due to their biocompatibility, superparamagnetic properties, controllable shape and size and scale-up capability.[23–25] These attractive features together with the nontoxic nature of SPIONs make magnetic nanoparticles ideal platforms for nanomedical applications, for example, as FDA approved contrast agents for MRI. Hence, SPIONs have widespread usage in various biomedical applications such as transfection, drug delivery, magnetic resonance imaging, cell/biomolecules separation and hyperthermia.[9,25,26]

In this work we focus on the interaction of SPIONs with a common plasma protein: iron saturated human transferrin protein. *To the best of our knowledge, this is the first report* *on conformational changes of a specific protein due to the interaction with SPIONs.*

Transferrin, with a molecular weight of 75–80 kDa depending on the species, is a protein which is found in the blood of all vertebrate species.[27] Transferrin contains two iron binding sites which appear to be equal and independent in their iron binding mode. As iron is bound to these sites, bicarbonate is bound to an anion binding site in close proximity to each of the iron binding sites, causing a red complex with an absorption at 465 nm.[28] Centrifugation has been used as the favoured method in order to separate the nanoparticles from the protein suspensions which can affect the outcome by the duration of washing and the amount of solution volumes used in these steps.[7] However, the main problem of the centrifugation technique is the loss of the proteins which are adsorbed to the nanoparticle surface with weak binding.[7,29] The distinguished feature of SPIONs is their superparamagnetic properties which enable us to separate them without centrifugation, using external magnetic field gradients; hence, more reliable results may be obtained.

The curvature of the nanoparticles surface can have a significant influence on the adsorption of biomolecules which can cause various conformational changes in protein structure adsorbed to flat surfaces of the same material.[14,29,30] To track the effect of various sizes on the transferrin conformational changes, both bare and polyvinyl alcohol (PVA) coated SPIONs, with 2 different particle sizes, were synthesized *via* an optimized co-precipitation method and characterized with TEM, XRD and VSM methods. In order to characterize the protein–SPIONs interactions, different techniques including circular dichroism (CD) spectro-polarimeter, fluorescence and UV/vis spectroscopy, and gel electrophoresis are employed.

2 Materials and methods

2.1 Materials

Analytical grade of iron salts (*i.e.* iron chloride) and sodium hydroxide (NaOH) were purchased from Merck Inc. (Darmstadt, Germany) and were employed without further purification. Polyvinyl alcohol (PVA) of 30 000–40 000 g mole^{-1} nominal molecular weight and 86–89% degree of hydrolysis was supplied by Fluka (Ronkonkoma, USA), respectively. Iron saturated human transferrin (purity of greater than 99%) with molecular weight of 77 kDa and a size of about 6 nm was prepared from Scipac (Kent, UK). The human transferrin was prepared from the human serum (fully tested and certified negative for HIV I and II antibodies, Hepatitis B surface antigen, and Hepatitis C antibodies). Other solvents were reagent grades and used without any further purification.

2.2 Synthesis of bare and coated SPIONs

After 20 minutes bubbling with neutral gas (*i.e.* argon), deoxygenated solutions were achieved using the de-ionized (DI) water. The iron salts (*i.e.* $FeCl_3$ and $FeCl_2$) were dissolved in deoxygenated DI water (1 M HCl), respectively. The iron solutions were mixed by adjusting to a molar fraction of 2 (Fe^{3+}/Fe^{2+}) for all samples. The nanoparticles were formed by drop wise addition of a predetermined mixture of iron salts to the base medium (NaOH) under an argon atmosphere. In order to achieve high monodisperse nanoparticles (decrease the mass transfer phenomena, which may allow nanoparticles to combine and build larger polycrystalline nanoparticles), the reactor was transferred to an ultrasonic bath (100 Watt) for creating a turbulent flow.[31] From data obtained by optimal uniform design,[31] two sets of samples with narrow size distributions were synthesized by variation of the base molarities and the homogenization rates. For both sets, the base molarities were adjusted to 1.2 whereas the homogenization rates were fixed at 10 800 rpm (batch 1) and 3600 rpm (batch 2) to achieve magnetic nanoparticles with two different sizes. After 30 min, the solutions were placed in a strong magnetic field gradient produced by a permanent Nd–Fe–B magnet (with cylindrical shape, diameter of 4 cm and height of 3 cm) and the SPIONs were collected. The supernatant was completely removed and the nanoparticles were re-dispersed in DI water several times. The permanent magnet was made of neodymium–iron–boron which exhibits superior magnetic properties.[32,33] The PVA solutions, with a polymer/iron mass ratio of 3, were added slowly to the colloidal dispersion of SPIONs (for both batches) by syringe (about 100 μl per drop) and kept stirred for another 1 h in order to coat the surface of the SPIONs. Single coated nanoparticles (no aggregation) can be achieved by adjusting the polymer/iron mass ratio.[34,35] The coated nanoparticles were collected by the magnet and re-dispersed in DI water. The washing procedure was repeated several times. Finally, the obtained ferrofluid was kept at 4 °C for protein-interaction experiments.

2.3 Interaction of SPIONs with protein

SPIONs were incubated with the iron saturated human transferrin protein for a period of 2 h at a temperature of 5 °C. The

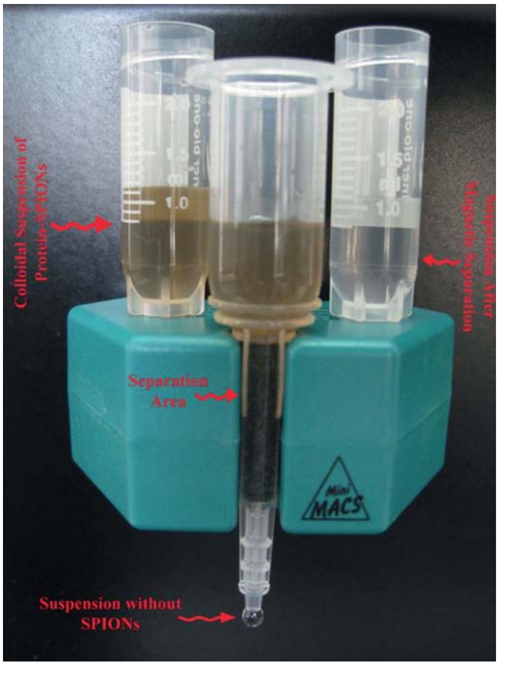

Fig. 1 Experimental setup for purification. The MACS® columns are composed of a spherical steel matrix; by inserting a column in a MACS Separator, a high-gradient magnetic field is induced within the column which retains the SPIONs.

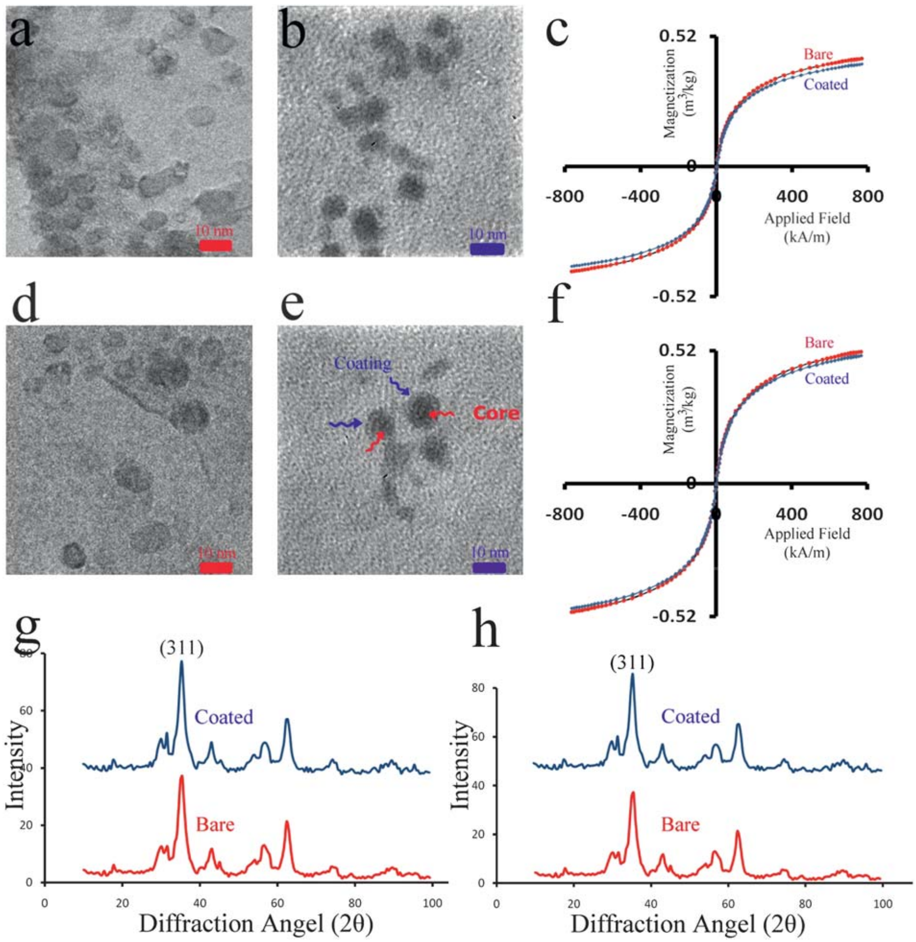

Fig. 2 (a and b) TEM images of batch 1 (homogenization rate of 10 800 rpm) for bare and coated SPIONs, respectively and (c) their corresponding VSM curves; (d and e) TEM images of batch 2 (homogenization rate of 3600 rpm) for bare and coated SPIONs, respectively and (f) their corresponding VSM curves; (g and h) XRD patterns of both batches for bare and coated SPIONs.

medium (30 times diluted with phosphate buffered saline (PBS); PBS was prepared according to the common preparation method[36] with a pH of 7.4) containing transferrin was incubated with the nanoparticles, with the protein solution to nanoparticle surface ratio fixed at 2.8 ml m^{-2} of SPIONs surface, in order to achieve a similar protein to nanoparticle surface ratio.[30] After the interaction time, the proteins with SPIONs were run through a strong magnetic field using a magnetic-activated cell sorting (MACS®), in order to trap the SPIONs in the magnetic column. Consequently, the flow-through fraction was collected and the trapped nanoparticles were washed with the 1 M KCl solution. The experimental setup is summarized in Fig. 1. The collected solutions, containing the interacted proteins, were analyzed by circular dichroism spectroscopy and SDS-PAGE (sodium dodecyl sulfate-polyacrylamide gel electrophoresis). Finally, the same procedure was employed for high concentrations (10 and 100 times) of SPIONs relative to the protein (*i.e.* by reducing the protein to nanoparticle surface ratio).

Nanoparticles were characterized as follows. After placing and drying a drop of the colloidal suspension of SPIONs on a copper grid, the size and shape of the magnetic nanoparticles were evaluated with a Phillips CM200 transmission electron

Table 1 Size for uncoated and coated SPIONs with the calculated thickness of transferrin on SPIONs surfaces

Batch	Bare/coated	Sample name	Average TEM size/nm	Average XRD size/nm	Average thickness of adsorbed protein measured by TEM size/nm
1 (homogenization rate: 10 800 rpm)	Bare	1B	5	3.6	1.6 ± 0.2[a]
	Coated	1C	8	3.5	3.8 ± 0.7[a]
2 (homogenization rate: 3600 rpm)	Bare	2B	8	5.3	4 ± 1[a]
	Coated	2C	10	5.3	4.4 ± 0.6[a]

[a] Obtained from an average of twenty separate TEM measurements of single transferrin coated nanoparticles; numbers given with the standard deviation.

Table 2 Description of sample abbreviations (*e.g.*, batch 1)

Sample	Description
B	Bare nanoparticles
C	PVA-Coated nanoparticles
BP	Protein interacted with bare nanoparticles
CP	Protein interacted with PVA-coated nanoparticles
BP-Mag	Extract of the interacted proteins with bare nanoparticles using MACS
CP-Mag	Extract of the interacted proteins with PVA-coated nanoparticles using MACS
BP-KCl	Washing of the trapped bare nanoparticles in MACS with 1 M KCl solution
CP-KCl	Washing of the trapped PVA-coated nanoparticles in MACS with 1 M KCl solution
N-BP	Extract of the bare nanoparticles from the MACS after washing
N-CP	Extract of the PVA-coated nanoparticles from the MACS after washing
BP-10	Using bare nanoparticles with 10 times concentration (protein amount is constant)
CP-10	Using PVA-coated nanoparticles with 10 times concentration (protein amount is constant)
BP-100	Using bare nanoparticles with 100 times concentration (protein amount is constant)
CP-100	Using PVA-coated nanoparticles with 100 times concentration (protein amount is constant)

microscope (TEM) equipped with an AMT 2 × 2 CCD camera at an accelerating voltage of 200 kV. Phase characterizations of the SPIONs were accomplished using XRD (Siemens, D5000, Germany) with Cu Kα radiation and the Scherrer method was employed for defining the average crystallite size of SPIONs. XRD samples were prepared by drying the nanoparticles in a vacuum oven at 40 °C for 12 h after magnetic separation. The magnetizations of the nanoparticles were measured in a vibrating sample magnetometer (VSM) with a sensitivity of 10^{-6} J T^{-1} emu^{-1} and a magnetic field up to 800 kA m^{-1}. The mean size of nanoparticles was determined by dynamic light scattering (DLS; Zetasizer model ZEN 1600, nano laser 633 nm). The removals of SPIONs from the solution were done by using magnetic columns (MACS; A Mini MACS® Separation Unit, Miltenyi Biotec Inc, Germany).

The CD-spectra of the human transferrin with a concentration of 0.5 mg ml^{-1} were obtained at room temperature using a Jasco J-810 spectro-polarimeter (Tokyo, Japan). The far-UV spectra were recorded using a step size of 2 nm and a bandwidth of 1.5

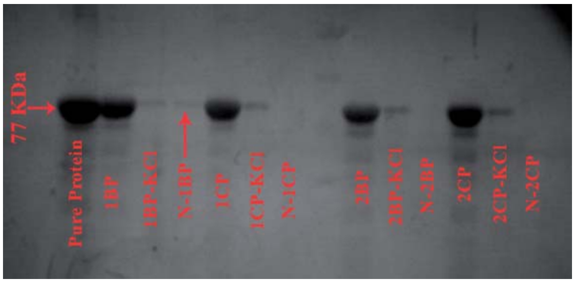

Fig. 4 SDS-PAGE for human transferrin and various separation solutions.

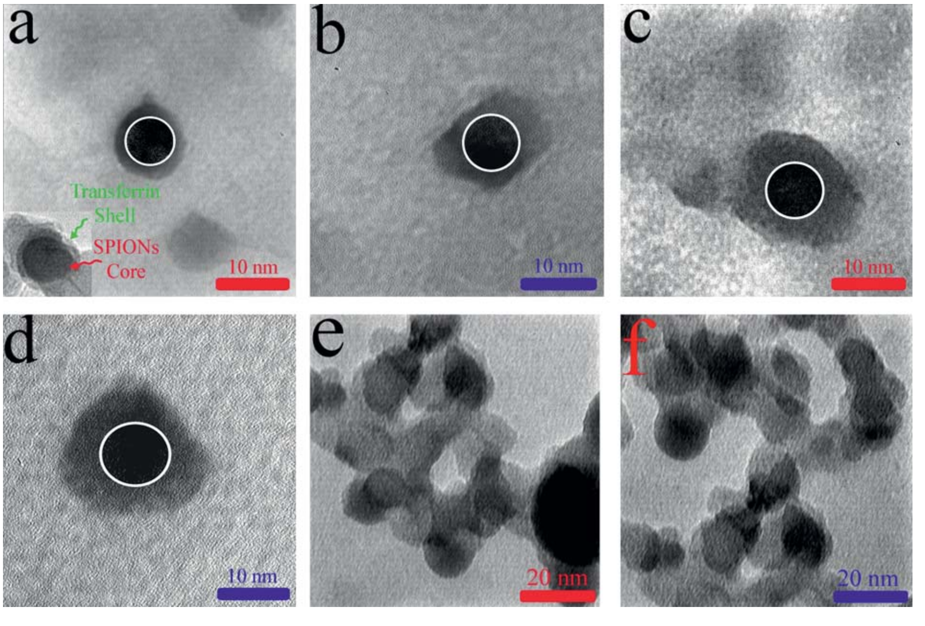

Fig. 3 (a and b) TEM images of transferrin corona coated SPIONs (batch 1) for bare and PVA-coated samples, respectively. Inset at the bottom left is the TEM image of a single protein-coated SPIONs showing lower density of the protein shell; (c and d) TEM images of transferrin corona coated SPIONs (batch 2) for bare and PVA-coated samples, respectively. The white circles are drawn as a guide for the eyes as a representation of the size of nanoparticles before protein adsorption; (e and f) TEM images of protein-coated SPIONs (bare and PVA-coated of batch 1) showing the agglomeration of these particles.

Table 3 Average size of the samples, with reduced protein to SPIONs surface ratio, were measured by DLS, 2 hours after interaction of SPIONs with transferrin

Batches	Sample name	Average hydrodynamic size/nm	Sample name	Average hydrodynamic size/nm	Sample name	Average hydrodynamic size/nm
1B	1B	8.2	1B-10	8.2	1B-100	8.2
	1BP	85.1 ± 12.6[a]	1BP-10	53.1 ± 10.3[a]	1BP-100	31.2 ± 1.2[a]
	N-1BP	25.3 ± 4.2[a]	N-1BP-10	42.3 ± 7.1[a]	N-1BP-100	27.5 ± 3.6[a]
1C	1C	12.6	1C-10	12.6	1C-100	12.6
	1CP	71.2 ± 11[a]	1CP-10	58.2 ± 10.1[a]	1CP-100	48.3 ± 8.9[a]
	N-1CP	16.3 ± 3.1[a]	N-1CP-10	37.1 ± 4.3[a]	N-1CP-100	41.3 ± 6.5[a]
2B	2B	12.1	2B-10	12.1	2B-100	12.1
	2BP	82.3 ± 15.4[a]	2BP-10	57.5 ± 13.1[a]	2BP-100	36.2 ± 5.9[a]
	N-2BP	18 ± 2.2[a]	N-2BP-10	39.4 ± 4.7[a]	N-2BP-100	31.6 ± 3.9[a]
2C	2C	15.3	2C-10	15.3	2C-100	15.3
	2CP	72 ± 18.2[a]	2CP-10	63.6 ± 11.1[a]	2CP-100	48.7 ± 10.4[a]
	N-2CP	21.7 ± 3.2[a]	N-2CP-10	35.2 ± 4.5[a]	N-2CP-100	39.4 ± 8.3[a]

[a] Obtained from an average of five separate DLS measurements where the uncertainty represents standard deviation.

nm. The spectra were recorded in a cell with a path length of 1 mm; the cell path length for far-UV spectra of 190–250 nm. The spectra were corrected for buffer contributions. The fluorescence spectra were recorded on a LS55 Fluorescence spectrometer (PerkinElmer, Belgium).

The denaturing polyacrylamide gel electrophoresis (SDS-PAGE) was performed following the procedure reported previously.[37]

3 Results and discussion

3.1 Bare and coated SPIONs

Fig. 2a–h show the characteristics for the SPIONs using TEM, XRD, and VSM techniques. TEM results (Fig. 2a and b (for batch 1), Fig. 2d and e (for batch 2)) confirm the formation of magnetite nanoparticles with spherical-shape and a narrow size distribution. Agglomeration is detectable in the bare nanoparticles (Fig. 2a and d) whereas for coated particles single coated nanoparticles are achieved. According to the TEM results, the size of nanoparticles is increased in the lower stirring rate. The colloidal stability of PVA coated SPIONs is higher than the stability of the bare particles because the former show steric stabilization. From the VSM curves (Fig. 2c and f), it can be concluded that both bare and coated nanoparticles have superparamagnetic properties with different magnetic saturations. The small difference is caused by the adsorbed layer of polymers which reduces the magnetic active mass of the particle to the total mass of the coated SPIONs. What is interesting is the difference of the magnetic saturation with increasing particle size. It has been recognized that the magnetic saturation of SPIONs increases when the size of the magnetite crystallite increases, which is attributed to the increase of the ratio of the magnetic active mass to the total volume of SPIONs.[38,39] The coating can not only cause a decline in exchange penetration as well as dipolar interactions but also cause the existence of a lower amount of iron (because magnetite is replaced by the non-magnetic polymer) together with creating magneto-crystalline anisotropy.[40] Fig. 2g and h illustrate the XRD spectra for all samples, which are matched well with magnetite (Fe_3O_4, reference JCPDS no. 82-1533), The full width at half maximum (FWHM) of the main reflection of magnetite (*i.e.* (311)) was employed, according to the Scherrer method, to determine the average crystallite size of the achieved nanoparticles (Table 1). In addition, the descriptions of sample abbreviations are presented in Table 2.

3.2 TEM investigation and SDS-PAGE gel electrophoresis

The SDS-PAGE is employed, following the protocol,[37] in order to track significant chain breaking in human transferrin due to the interaction with the nanoparticles. The role of SDS is the disruption of hydrophobic areas of the protein structure and coating the proteins with negative charges, causing the formation of linearized protein. The variation of protein conformations cannot interfere with the chain breaking. To give qualitative support for the broader conclusions, the TEM data for all particles before and after interaction with human transferrin are compared (Fig. 2a, b, d, e and 3). Since particle agglomeration occurs, after protein adsorption on the surface of nanoparticles,[14] the polydispersity of SPIONs in size and the protein conformation need to be interpreted carefully. For this purpose, the TEM investigations of single SPIONs–transferrin complexes are used to compute the thickness of the protein which is adsorbed to the surface of SPIONs according to a simple core–shell model (see Fig. 3 and Table 1). The selected images (Fig. 3) illustrate clear evidence of a thin transferrin-derived layer around the SPIONs following incubation with human transferrin protein. These adsorbed layers completely coat the particles and also coat the particles involved in larger aggregates (see Fig. 3e and f).

In order to define the polydispersity of the thickness of protein coating on the surface of SPIONs, statistics are applied.[41]

According to Fig. 3 and Table 1, the shape and thickness of adsorbed transferrin to the surface of SPIONs are significantly related to their surface curvature and modifications (*i.e.* bare or PVA-coated). The obtained results are in good agreement with the thickness of the human serum albumin on ultra-small (10–20 nm in diameter) polymer-coated FePt and CdSe/ZnS nanoparticles.[18] Using fluorescence correlation spectroscopy together with the assumption of Stokes–Einstein diffusion, it was found

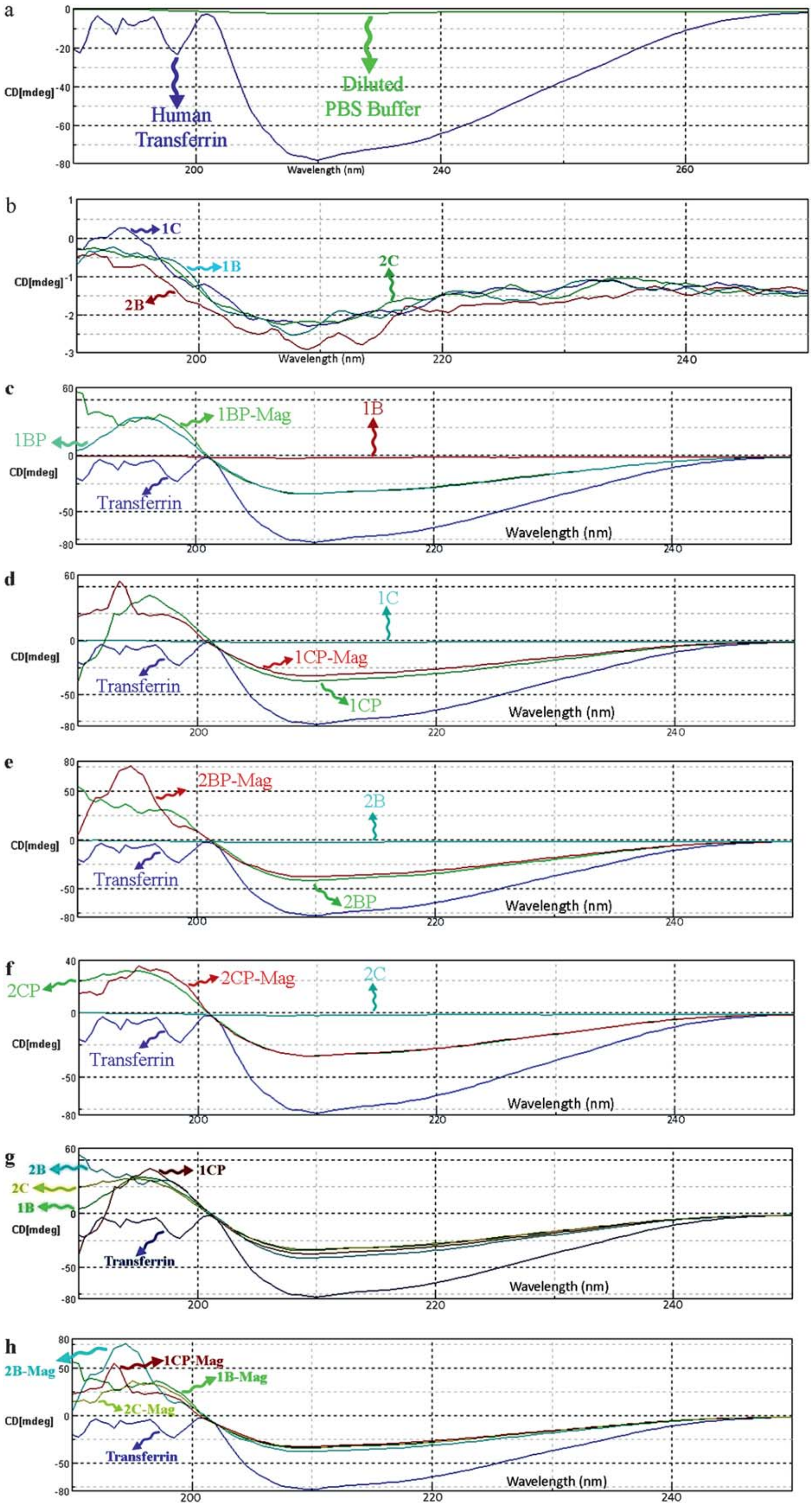

Fig. 5 CD spectra of (a) pure human transferrin (iron saturated) and buffer medium; (b) various magnetic nanoparticles CD spectra of pure human transferrin, SPIONs, suspension of transferrin and SPIONs nanoparticles, and pure treated transferrin after MACS magnetic separation for (c) 1B, (d) 1C, (e) 2B, and (f) 2C samples; comparison of CD spectra of (g) suspensions containing transferrin and SPIONs nanoparticles, and (h) suspensions after MACS magnetic separation.

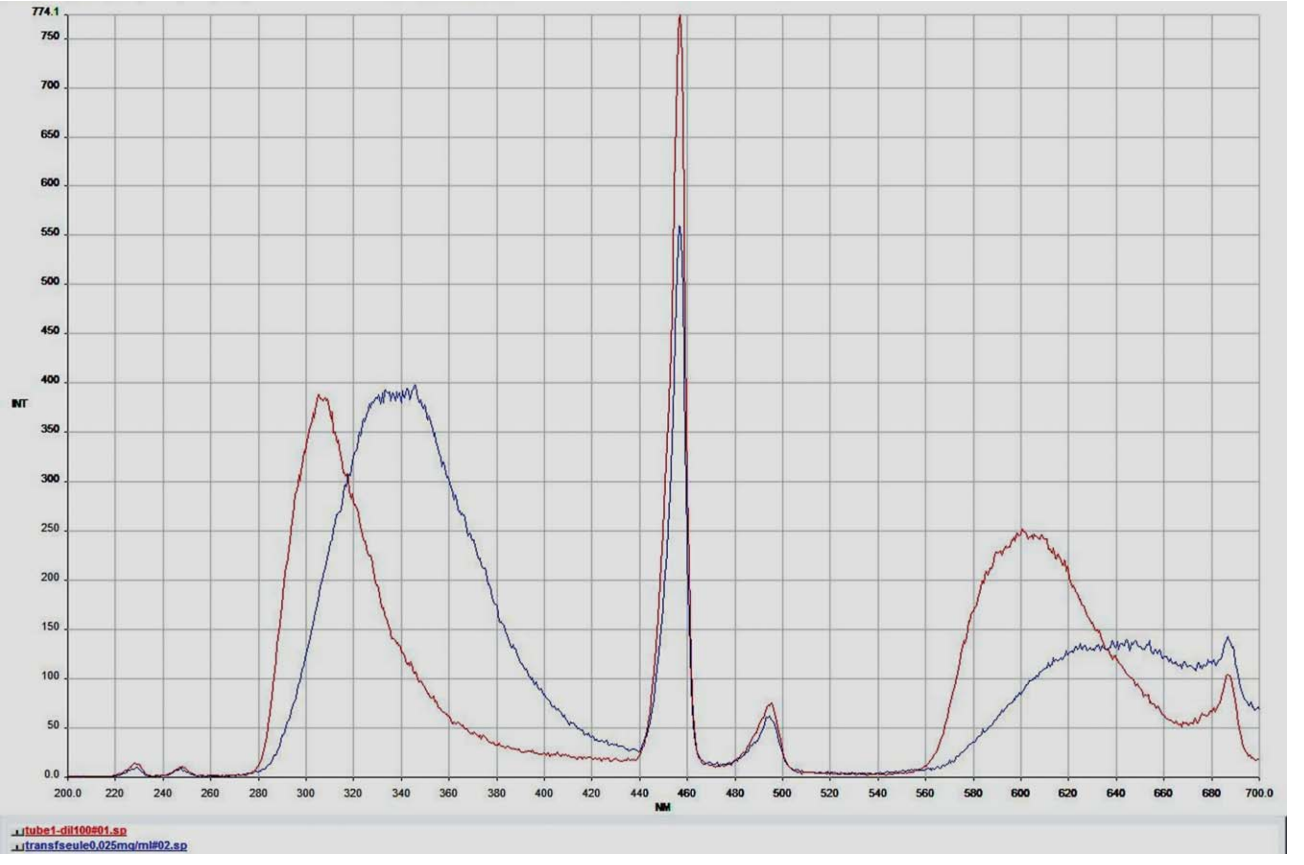

Fig. 6 Comparison of fluorescence spectra of pure human transferrin solution (25 μg ml^{-1}, blue curve) and of pure treated transferrin after MACS magnetic separation (red curve).

that the increase in the nanoparticle size after the binding of albumin is consistent with the saturation binding of a monolayer with a thickness of 3.3 nm.[18]

The protein-interacted SPIONs were fixed in MACS beads; consequently, the flow-through solution obtained from the fixed SPIONs, and the washing of the fixed SPIONs with 1M KCl solution, are collected and analysed by SDS-PAGE. Human transferrin shows a tight cluster of bands corresponding to the transferrin molecular weight of 77 kDa (Fig. 4). According to Fig. 4, there is no detectable protein breaking due to the interaction with the magnetic nanoparticles. Probing the bands in 1 M KCl solutions reveals the attachment tendency of human transferrin to both bare and coated SPIONs in the two batches. After washing with KCl solution, the fixed SPIONs are collected by removing the column from the high magnetic field and then are analysed with gel electrophoresis. A trace of protein attachment to N-1BP sample is detected even after washing with KCl solution, whereas there is no detectable band in other nanoparticles, confirming the strong interaction between human transferrin and smaller bare SPIONs (diameter of 5 nm). The attachment of human transferrin to the SPIONs is highly dependent on both the size and the surface coating of the magnetic nanoparticles which is confirmed by the DLS results (Table 3). The change of the size of the SPIONs is not only related to the adsorption of the transferrin but also can be explained by the agglomeration of the protein coated SPIONs. More specifically, from the DLS data, it is observed that the effective "size" of the nanoparticles increases dramatically as they become coated with the protein and then begin to aggregate due to the presence of this coating. The nanoparticle clustering is directly apparent in TEM images of SPIONs after exposure to the human transferrin (Fig. 3e and f). Similar results have been obtained for gold nanoparticles after absorbance of common human blood proteins such as albumin, fibrinogen, γ-globulin, histone, and insulin.[42]

3.3 CD spectra and UV/vis spectroscopy

3.3.1 Protein to nanoparticle surface ratio. All samples were analysed by CD spectra in order to track the changes in protein conformation due to the interaction with magnetic nanoparticles. The CD spectrum and UV/vis results of the pure human transferrin (iron saturated) and the buffer medium (30 times diluted phosphate buffer saline) are shown in Fig. 5a. The CD spectra of the human transferrin confirm the existence of its closed compact conformation. Human serum transferrin is composed of two similar, but non-identical globular lobes, and each lobe (which houses an Fe(III)-binding site in a cleft between its domains)[43,44] is divided into two domains consisting of β-sheets overlaid with α-helices.[45–47] By releasing the iron from the transferrin structure (apotransferrin), the compact conformation is relaxed, more specifically the two domains of each lobe are going to achieve an open jaw conformation.[48] CD spectra of the diluted PBS and all SPIONs (Fig. 5b) show curves near zero base line confirming their negligible effect on the CD spectra.

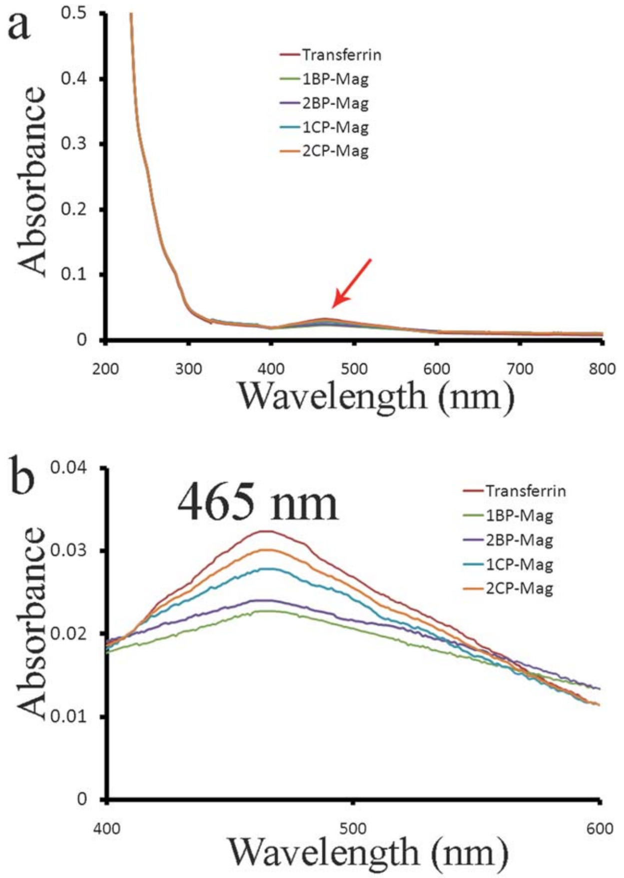

Fig. 7 (a) UV/vis spectroscopy showing the absorbance changes associated with iron release for the SPIONs-treated transferrin due to their conformation changes and (b) showing the peaks of (a) in the 400–600 nm range.

The CD spectra show that by introducing SPIONs to transferrin solution (Fig. 5c–h), the conformation of the iron saturated protein is changed. The significant decline in peak intensity at the wavelength of around 210 nm for the interacted proteins confirms the opening of the compact transferrin conformation. After removing the magnetic nanoparticles using the MACS system, the original conformation of the proteins is not recovered, showing the irreversible changes in transferrin conformation after interaction with the SPIONs (Fig. 5h).

These results are also confirmed by the fluorescence studies. The fluorescence spectra of the protein alone and of the protein after interactions with SPIONs were compared (Fig. 6). A shift for the λ_{max} of the emission (340 nm for the ZZ protein alone and 310 nm for the protein after interaction with the SPIONs) was observed. This difference clearly indicates a conformational change of the protein.

The UV/vis spectroscopy of the pure transferrin and SPIONs-treated pure transferrin after removing SPIONs are illustrated in Fig. 7a and b. The characteristic peak at the wavelength of 465 nm is due to the iron-bearing lobes of iron saturated transferrin. Therefore, the release of iron from the two tyrosine ligands causes a decline in the peak.[49,50] According to the CD curves, the exposure of iron saturated human transferrin to SPIONs results in the release of iron, and more specifically, it changes the compact conformation to the open conformation of the iron-free lobe. Furthermore, the decline in the characteristic peak of the transferrin (at 465 nm) is dependent on the size and surface properties of SPIONs. For instance, the most significant protein conformational changes are obtained by its interaction with the bare nanoparticles (*i.e.* 1B). The PVA-coated nanoparticles cause less conformation changes in transferrin, probably due to its lower surface energy in comparison to the bare magnetic nanoparticles; the same effects of the size of SPIONs are detected in coated nanoparticles.

3.3.2 Reduction of the protein to nanoparticle surface ratio. By increasing the SPIONs' concentrations (by a factor of 10 and 100 times) for all samples, more change in the conformation of transferrin can be observed (Fig. 8a–d). A significant decline in peaks at 210 nm occurs by increasing the SPIONs' concentration. The conformation changes are irreversible, since the original conformations of pure nanoparticle-treated proteins are not recovered after removal of the SPIONs using the MACS system (Fig. 8e–h). The reason may be attributed to the release of Fe(III) ion from the transferrin structure which is consistent with the UV/vis results. The DLS analyses (Table 3) are employed in order to investigate the effect of the protein to nanoparticle surface ratio on the interaction nature of transferrin and magnetic nanoparticles. A significant reduction in the particle size of the protein to nanoparticle surface ratio is observed not only in protein–nanoparticle solution, but also in pure treated protein after removal of SPIONs using MACS. It appears that weaker binding exists for the higher ratio of protein to nanoparticles surface, compared to the lower ratios (for 10 and 100 fold particle increase), due to the ratio of the surface energy of nanoparticles to the number of proteins. By decreasing the ratio of the protein to nanoparticle surface, the numbers of proteins per nanoparticles are significantly decreased; therefore, more energy is transferred from the nanoparticles to each protein molecule causing stronger binding, leading to more conformational changes between proteins and nanoparticles. Hence, the observed significant decrease in the hydrodynamic size of the higher ratio of protein to nanoparticle surface is due to the weak binding that causes the release of interacted protein after MACS separation. On the other hand, for the lower ratios, the stronger binding between protein and nanoparticles does not allow proteins to be released during the magnetic separation method. A possible mechanism is illustrated in Fig. 9. In order to support the hypothesis, SDS-PAGE gel electrophoresis was employed (Fig. 10). The results suggest that by decreasing the protein to SPIONs surface ratio, the remaining proteins on the surface of SPIONs (after separation of magnetic nanoparticles with MACS) are increased significantly, due to the enhancement of the binding energy between protein and SPIONs. Interestingly, the band widths of the proteins are decreased for the PVA-coated nanoparticles. In addition, DLS results confirm the hypothesis (Table 3). From the results, it is found for the first time that beside the physiochemical properties of nanoparticles, their concentration can have an important impact on the "protein corona", *i.e.*, changing the soft corona to a hard corona. By increasing the concentration of the SPIONs, a harder corona is created on the surface of nanoparticles (see bands in Fig. 10). The reduction of the hydrodynamic size of protein coated nanoparticles, as seen in the DLS data, confirms that by increasing the

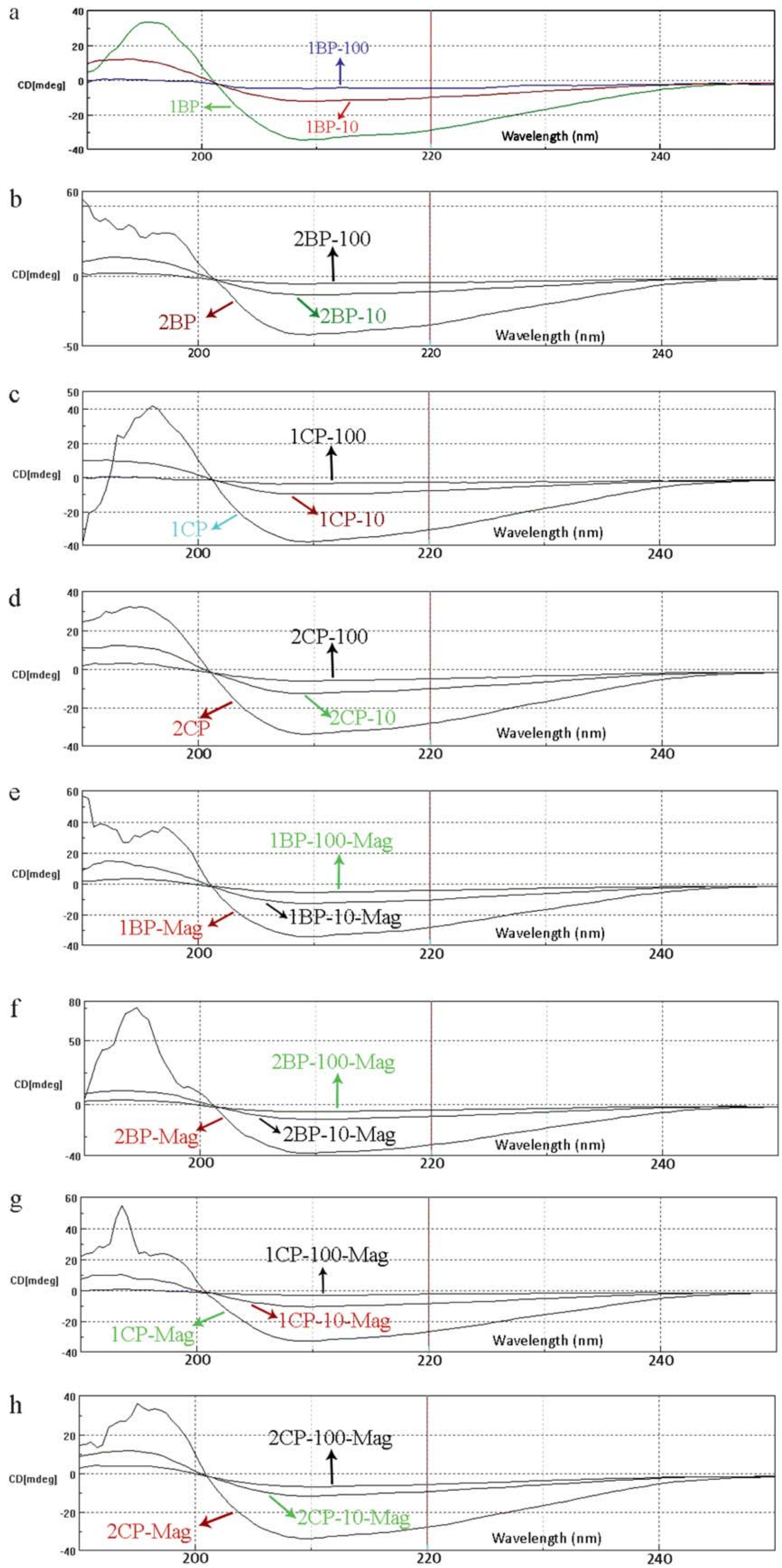

Fig. 8 CD spectra of protein–nanoparticle solution with various SPIONs concentrations for (a) 1B, (b) 2B, (c) 1C and, (d) 2C samples; CD spectra of pure treated protein after removal of SPIONs (with various concentrations) by MACS for (e) 1B, (f) 2B, (g) 1C and (h) 2C samples.

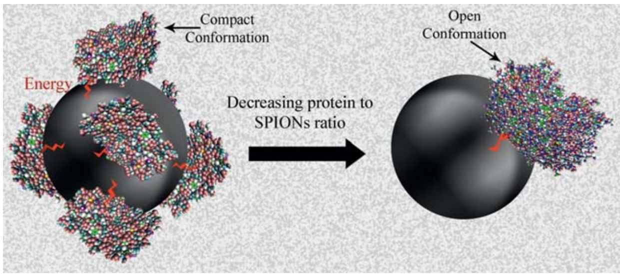

Fig. 9 Schematic representation of the decreasing protein effect to SPIONs surface ratio on the conformation changes in human transferrin.

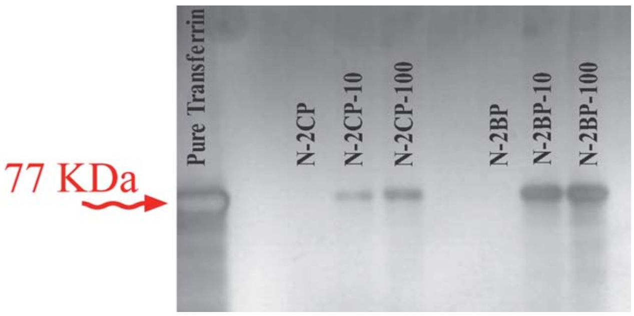

Fig. 10 SDS-PAGE for human transferrin and remained proteins on the surface of trapped bare- and coated-SPIONs (with various concentrations).

SPIONs concentration, not only are the attachment of proteins stronger (increasing of conformational changes from compact to open structure), but also the thickness of the protein corona is decreased (due to the reduction of protein to SPIONs surface ratio). Furthermore, by removing the protein from the SPION surface by using various washing solutions, it is seen that the hydrodynamic size of SPIONs with high concentrations are bigger than the lower ones, indicating a stronger attachment of protein to SPIONs (Table 3 and Fig. 9). The agglomeration of protein coated SPIONs has a reverse proportion to the concentration of SPIONs (less agglomeration at higher concentration). We hypothesize that the extensive conformational changes of transferrin on the SPION surface with high concentrations could reduce the affinity of surface proteins to bind each other, causing less agglomeration.

UV/vis results (Fig. 11a–d) confirm the enhancement of the iron release from the transferrin molecules due to its conformation changes by increasing the SPIONs concentration (decreasing the protein to SPIONs surface ratio), which fully agrees with our schematic hypothesis (Fig. 9). In addition, there is no peak for the lowest applied ratio, for all samples, showing the almost complete transition of iron saturated human transferrin from the closed conformation to the open jaw conformation. The iron release from the coated SPIONs is lower than the bare SPIONs for the higher protein to SPIONs surface ratio; however there are no differences for the lowest ratio.

4 Conclusion

Both bare and PVA coated SPIONs, with 2 different particle sizes, were synthesized *via* optimized co-precipitation method and characterized with TEM, XRD and VSM methods. The SPIONs were incubated with iron saturated human transferrin protein. After incubation, the mixture was run through a column placed in a strong magnetic field and was washed with KCl solution to elute the protein. The solutions containing the

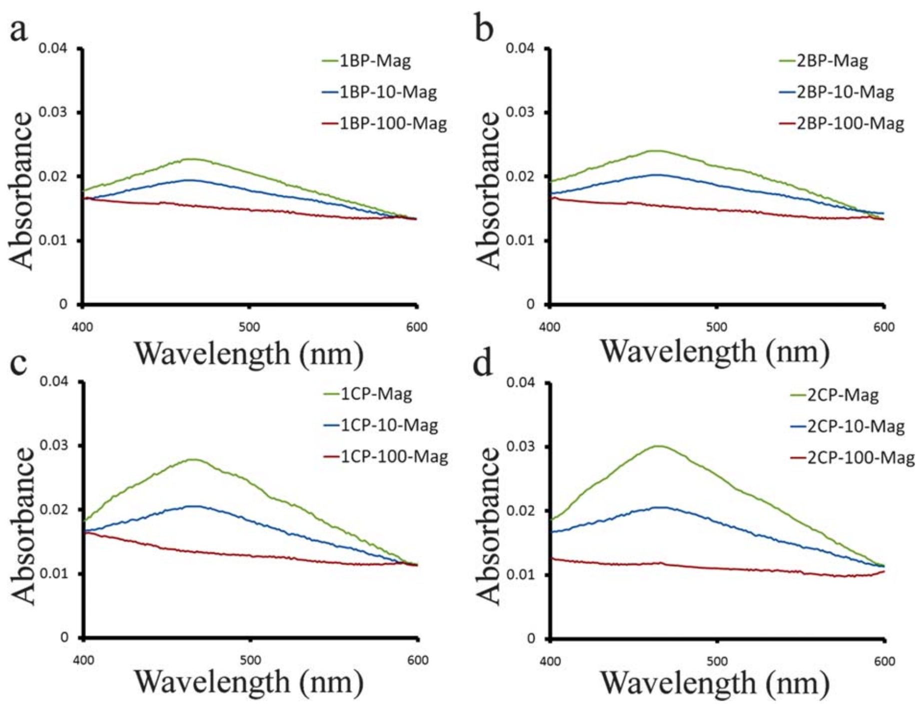

Fig. 11 UV/vis results of pure treated protein after removal of SPIONs (with various concentrations) by MACS for (a) 1B, (b) 2B, (c) 1C and (d) 2C samples.

proteins which interacted with the SPIONs were analyzed by fluorescence and UV/vis spectroscopy, SDS-PAGE gel electrophoresis and circular dichroism. Our results show that the conformation of the iron saturated transferrin is changed due to the interaction with SPIONs. The conformation of the pure protein is not recovered, indicating irreversible changes in transferrin conformation after this interaction. The human transferrin conformational change from a compact structure to a more open jaw structure is due to the loss of iron. This is the first published report on the irreversible conformational changes of a specific protein due to the interaction with SPIONs.

References

1 M. Nirmal and L. Brus, Luminescence photophysics in semiconductor nanocrystals, *Acc. Chem. Res.*, 1999, **32**, 407–414.
2 A. P. Alivisatos, Semiconductor clusters, nanocrystals, and quantum dots, *Science*, 1996, **271**, 933–937.
3 W. C. W. Chan and S. Nie, Quantum dot bioconjugates for ultrasensitive nonisotopic detection, *Science*, 1998, **281**, 2016–2018.
4 Y. Weng, Nonlinear optical properties of nanometer-sized semiconductor clusters, *Acc. Chem. Res.*, 1991, **24**, 133–139.
5 M. L. Steigerwald and L. E. Brus, Semiconductor crystallites: a class of large molecules, *Acc. Chem. Res.*, 1990, **23**, 183–188.
6 D. Alloyeau, et al. Size and shape effects on the order–disorder phase transition in CoPt nanoparticles, *Nat. Mater.*, 2009, **8**, 940–946.
7 T. Cedervall, et al. Understanding the nanoparticle–protein corona using methods to quantify exchange rates and affinities of proteins for nanoparticles, *Proc. Natl. Acad. Sci. U. S. A.*, 2007, **104**, 2050–2055.
8 I. Lynch, et al. The nanoparticle–protein complex as a biological entity; a complex fluids and surface science challenge for the 21st century, *Adv. Colloid Interface Sci.*, 2007, **134–135**, 167–174.
9 M. Mahmoudi, et al. A new approach for the *in vitro* identification of the cytotoxicity of superparamagnetic iron oxide nanoparticles, *Colloids Surf., B*, 2010, **75**, 300–309.
10 M. Mahmoudi, A. Simchi and M. Imani, Cytotoxicity of uncoated and polyvinyl alcohol coated superparamagnetic iron oxide nanoparticles, *J. Phys. Chem. C*, 2009, **113**, 9573–9580, DOI: 10.1021/jp9001516.
11 T. Cedervall, et al. Detailed identification of plasma proteins adsorbed on copolymer nanoparticles, *Angew. Chem., Int. Ed.*, 2007, **46**, 5754–5756.
12 I. lynch, A. Salvati and K. A. Dawson, Protein–nanoparticle interactions: what does the cell see?, *Nat. Nanotechnol.*, 2009, **4**, 546–547.
13 K. A. Dawson, A. Salvati and I. Lynch, Nanotoxicology: nanoparticles reconstruct lipids, *Nat. Nanotechnol.*, 2009, **4**, 84–85.
14 D. Walczyk, F. B. Bombelli, M. P. Monopoli, I. Lynch and K. A. Dawson, What the cell "sees" in bionanoscience, *J. Am. Chem. Soc.*, 2010, **132**, 5761–5768.
15 A. E. Nel, et al. Understanding biophysicochemical interactions at the nano–bio interface, *Nat. Mater.*, 2009, **8**, 543–557.
16 M. S. Ehrenberg, A. E. Friedman, J. N. Finkelstein, G. Oberdörster and J. L. McGrath, The influence of protein adsorption on nanoparticle association with cultured endothelial cells, *Biomaterials*, 2009, **30**, 603–610.
17 T. A. Faunce, J. White and K. I. Matthaei, Integrated research into the nanoparticle-protein corona: a new focus for safe, sustainable and equitable development of nanomedicines, *Nanomedicine*, 2008, **3**, 859–866.
18 C. Röcker, M. Pötzl, F. Zhang, W. J. Parak and G. U. Nienhaus, A quantitative fluorescence study of protein monolayer formation on colloidal nanoparticles, *Nat. Nanotechnol.*, 2009, **49**, 577–580.
19 I. Lynch, K. A. Dawson and S. Linse, Detecting cryptic epitopes created by nanoparticles, *Science*, 2006, **327**, 14.
20 A. Nel, T. Xia, L. Madler and N. Li, Toxic potential of materials at the nanolevel, *Science*, 2006, **311**, 622–627.
21 D. B. Warheit, T. R. Webb, C. M. Sayes, V. L. Colvin and K. L. Reed, Pulmonary instillation studies with nanoscale TiO_2 rods and dots in rats: toxicity is not dependent upon particle size and surface Area, *Toxicol. Sci.*, 2006, **91**, 227–236.
22 V. L. Colvin, The potential environmental impact of engineered nanomaterials, *Nat. Biotechnol.*, 2003, **21**, 1166–1170.
23 M. Mahmoudi, et al. MRI tracking of stem cells *in vivo* using iron oxide nanoparticles asa tool for the advancement of clinical regenerative medicine, *Chem. Rev.*, 2010, DOI: 10.1021/cr1001832.
24 M. Mahmoudi, A. S. Milani and P. Stroeve, Surface architecture of superparamagnetic iron oxide nanoparticles for application in drug delivery and their biological response: a review, *International Journal of Biomedical Nanoscience and Nanotechnology*, 2010, **1**(2/3/4), 164–201.
25 M. Mahmoudi, S. Sant, B. Wang, S. Laurent and T. Sen, Superparamagnetic iron oxide nanoparticles (SPIONs): development, surface modification and applications in chemotherapy, *Adv. Drug Delivery Rev.*, 2010, DOI: 10.1016/j.addr., DOI: 10.1016/j.addr., in press.
26 M. Mahmoudi, A. Simchi, M. Imani, A. S. Milani and P. Stroeve, An *in vitro* study of bare and poly(ethylene glycol)-*co*-fumarate-coated superparamagnetic iron oxide nanoparticles: a new toxicity identification procedure, *Nanotechnology*, 2009, **20**(22), 225104.
27 D. G. Makey and U. S. Seal, The detection of four molecular forms of human transferrin during the iron binding process, *Biochim. Biophys. Acta*, 1976, **453**, 250–256.
28 P. Aisen, *Inorganic Chemistry*, American Elsevier, New York, 1973, ch. 9.
29 I. Lynch and K. A. Dawson, Protein–nanoparticle interactions, *Nano Today*, 2008, **3**, 40–47.
30 M. Lundqvist, et al. Nanoparticle size and surface properties determine the protein corona with possible implications for biological impacts, *Proc. Natl. Acad. Sci. U. S. A.*, 2008, **105**, 14265–14270.
31 M. Mahmoudi, A. Simchi, M. Imani, A. S. Milani and P. Stroeve, Optimal design and characterization of superparamagnetic iron oxide nanoparticles coated with polyvinyl alcohol for targeted delivery and imaging, *J. Phys. Chem. B*, 2008, **112**, 14470–14481.
32 T. Neuberger, B. Schopf, H. Hofmann, M. Hofmann and B. Rechenberg, Superparamagnetic nanoparticles for biomedical applications: possibilities and limitations of a new drug delivery system, *J. Magn. Magn. Mater.*, 2005, **293**, 483–496.
33 M. Arruebo, R. Fernandez-Pacheco, M. R. Ibarra and J. Santamaria, Magnetic nanoparticles for drug delivery, *Nano Today*, 2007, **2**, 22–32.
34 M. Mahmoudi, A. Simchi, A. S. Milani and P. Stroeve, Cell toxicity of superparamagnetic iron oxide nanoparticles, *J. Colloid Interface Sci.*, 2009, **336**, 510–518.
35 A. Chastellain, A. Petri and H. Hofmann, Particle size investigations of a multistep synthesis of PVA coated superparamagnetic nanoparticles, *J. Colloid Interface Sci.*, 2004, **278**, 353–360, DOI: 10.1016/j.jcis.2004.06.025.
36 R. Dulbecco and M. Vogt, Plaque formation and isolation of pure lines with poliomyelitis viruses, *J. Exp. Med.*, 1954, **99**, 167–182.
37 U. K. Laemmli, Cleavage of structural proteins during the assembly of the head of bacteriophage T4, *Nature*, 1970, **227**, 680–685.
38 J. Sun, et al. Synthesis and characterization of biocompatible Fe_3O_4 nanoparticles, *J. Biomed. Mater. Res., Part A*, 2007, **80**, 333–341.
39 P. S. Haddad, et al. Structural and morphological investigation of magnetic nanoparticles based on iron oxides for biomedical applications, *Mater. Sci. Eng., C*, 2008, **28**, 489–494.
40 M. Mahmoudi, A. Simchi, M. Imani and U. O. Hafeli, Superparamagnetic iron oxide nanoparticles with rigid cross-linked polyethylene glycol fumarate coating for application in imaging and drug delivery, *J. Phys. Chem. C*, 2009, **113**, 8124–8131.
41 W. E. Biles and J. J. Swain, *Optimization and Industrial Experimentation*, Wiley, New York, 1980.
42 S. H. De Paoli Lacerda *et al*, Interaction of gold nanoparticles with common human blood proteins, *ACS Nano*, 2009, **4**, 365–379.
43 B. F. Anderson, H. M. Baker, G. E. Norris, D. W. Rice and E. N. Baker, Structure of human lactoferrin: crystallographic structure analysis and refinement at 2.8 Å resolution, *J. Mol. Biol.*, 1989, **209**, 711–734.
44 M. S. Shongwe, et al. Anion binding by human lactoferrin: results from crystallographic and physicochemical studies, *Biochemistry*, 1992, **31**, 4451–4458.
45 B. F. Anderson, H. M. Baker and E. J. Dodson, Structure of human lactoferrin at 3.2-Å resolution, *Proc. Natl. Acad. Sci. U. S. A.*, 1987, **84**, 1769–1773.

46 C. T. Bailey, M. G. Patch and C. J. Carrano, Affinity labels for the anion-binding site in ovotransferrin, *Biochemistry*, 1988, **27**, 6276–6282.
47 E. N. Baker and P. F. Lindley, New perspectives on the structure and function of transferrins, *J. Inorg. Biochem.*, 1992, **47**, 147–160.
48 M. S. Navati, U. Samuni, P. Aisen and J. M. Friedman, Binding and release of iron by gel-encapsulated human transferrin: evidence for a conformational search, *Proc. Natl. Acad. Sci. U. S. A.*, 2003, **100**, 3832–3837.
49 M. G. Patch and C. J. Carrano, The origin of the visible absorption in metal transferrins, *Inorg. Chim. Acta*, 1981, **56**, L71–L73.
50 J. G. Grossmann, et al. Metal-induced conformational changes in transferrins, *J. Mol. Biol.*, 1993, **229**, 585–590.

